

# A Complete Study of Variability in Time and Amplitude of a Standard ECG Database

Manuel M. Casas, Roberto L. Avitia, Alexandra Gomez-Caraveo, Marco A. Reyna, and Jose A. Cardenas-Haro

**Abstract**—Currently the Electrocardiogram (ECG) is still an important and conventional tool that represents a pre-diagnosis system in a wide variety of heart diseases. Conventional Electrocardiography pre-diagnosis is based on time variations and ECG waveforms characteristics. Because of this, there are many studies and tables that describe time variations as heart healthy patterns, but there are almost no waveform amplitude variation studies that describe heart healthy patterns in an ECG trace. We reported here a complete evaluation of time and amplitude variations described by a very used ECG database called The PTB Diagnostic ECG Database. In order to measure ECG waveforms patterns in time and amplitude, we used a slightly modified and classic algorithm developed by Pan and Tompkins, as well as a proposed method based on wavelets. Results show complete descriptive tables that represent a heart-healthy subject both in time amplitude variations.

**Index Terms**—ECG trace, amplitude variability, time variability, ECG parameters.

## I. INTRODUCTION

Electrocardiogram or simply ECG trace is still an important pre-diagnosis tool that is continuously studied. Some researchers have developed many techniques and methods to interpret ECG as normal or abnormal based on professional experiences [1]. To classify an ECG as normal or abnormal, professional analyzes carefully characteristic waveforms called P wave, QRS complex, ST segment and T wave. A Normal Sinus Rhythm is reflective of a normally functioning conduction system, and an experimented physician can determine it looking the ECG trace and some parameters such as Rhythm, Rate, P wave configuration, PR interval and QRS duration and configuration [2], [3]. On the other hand, some authors have shown that waveforms (e.g. Q waves or ST segments) can mimic another kind of cardiac anomaly such as left bundle branch block or Hyperkalemia [4], [5], making ECG interpretation a diagnosis completely based on physician experience not a quantitative or automatic diagnosis. In this work, we classified the Normal Sinus Rhythm as a quantitative description in time and amplitude. We utilized the PTB Diagnostic ECG Database (PTBDED) and only that ECG traces considered as normal [6]. We used a

Manuscript received March 15, 2014; revised June 1, 2014. This work was supported in part by Seventeenth Internal Research Call for Research Projects from Autonomous University of Baja California under Grant 105/6/C/CC/17.

Manuel M. Casas is with the Mexican-European Institute of Sciences, Mexicali, ZP 21100, Mexico (e-mail: manuel.martinez.casas@gmail.com).

Roberto L. Avitia, Alexandra Gomez, Marco A. Reyna, and Jose A. Cardenas-Haro are with the Department of Bioengineering and Environmental Health, Autonomous University of Baja California, Mexicali, ZP 21100, Mexico (e-mail: ravitia@uabc.edu.mx).

classic and slightly modified Pan and Tompkins algorithm [7] to calculate the ECG parameters in time and a proposed method based on Wavelets to calculate the ECG parameters in amplitude. Results show a complete description in time and amplitude of that ECG traces considered as Normal Sinus Rhythm.

## II. MATERIALS AND METHODS

The PTBDED is part of Physionet databases that offers free access via the web to large collections of recorded physiologic signals. We selected the best defined 36 three Frank lead ECGs (X, Y, Z) with a sample rate of 1000 samples per second and aged 17 to 87. We localized those ECG segments considered as normal by the database (i.e. about 380 beats each orthogonal ECG traces) and those were characterized in time and amplitude as follow:

### A. Classification in Time of Normal ECG Traces

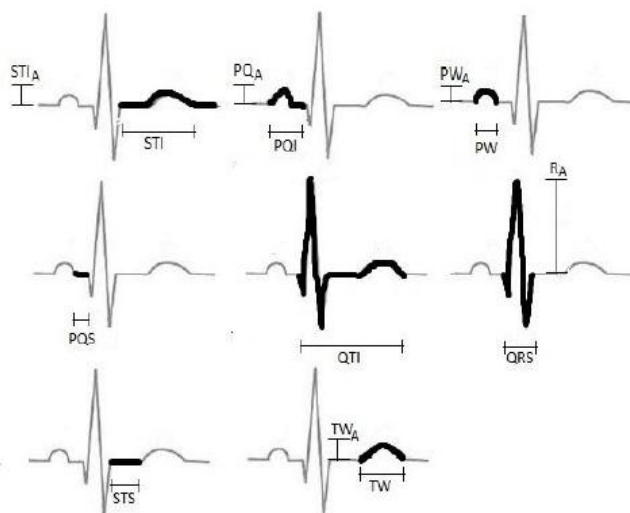


Fig. 1. Time and amplitude parameters taken in consideration to compute the ECG variability for the X and Y leads.

After ECG trace selection based on low noise signals (visual criterion), we classified each ECG trace in time-duration by the mean of the parameters described as: ST segment (STS), PQ interval (PQI), P wave (PW), PQ segment (PQS), QT interval (QTI), QRS complex (QRS), ST-T complex (STI) and T wave (TW) as shown in Fig. 1.

ECG traces were smoothed with a simple moving averaged filter of three points (assuring ECG bandwidth was not affected) and adjusted to an isoelectric baseline using a MATLAB® function msbackadj as shown in Fig. 2.

In order to calculate the beginning and the ending of the QRS complex (QRSon and QRSoft respectively), a slightly

modified of classical Pan and Tompkins algorithm was applied. This algorithm involves two filters that act as a band-pass filter (5-15 Hz) and a differentiation process that enhance the QRS complex and provides information of the slope. After this differentiation process, the QRS is squared to heighten much more the higher frequencies in the complete ECG trace. A moving integration window gives information to detect the QRSON and QRSoFF as shown in Fig. 3.

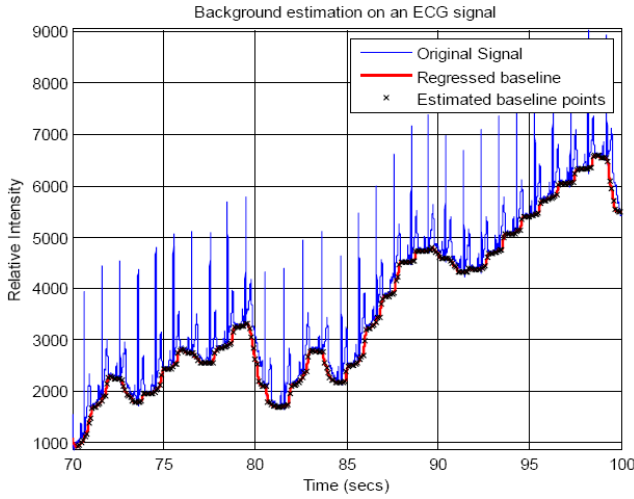


Fig. 2. Background estimation of an ECG with variable isoelectric line by applying *msbackadj* function. It permits to adjust each ECG trace to a constant isoelectric line.

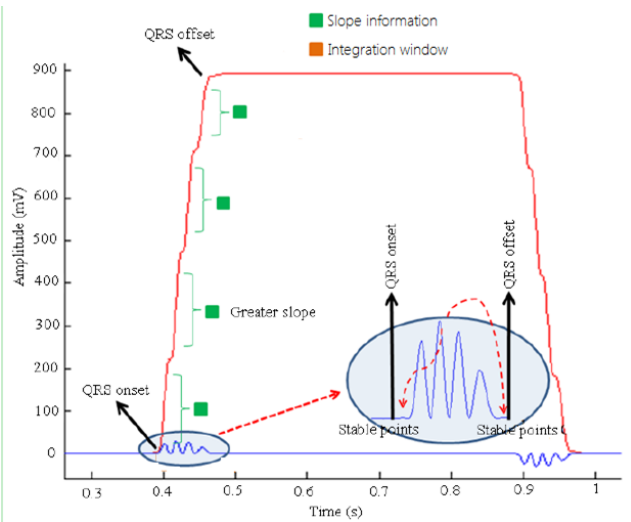


Fig. 3. Integration windows used to calculate QRSONset and QRSoFFset for each ECG trace. Slope calculation of the integration window give us the QRS duration.

Once we found QRSON and QRSoFF the difference between them was defined as QRS complex duration in ms or simply QRS. STS was computed from the QRSoFF to the time where the T wave slope starts to increase, and we calculated the TW when this slope finished to decrease. STI was defined adding STS+TW and QTI was found adding QRS+STS. PQS was established with the time when P wave finished decreasing to the time when QRSON occurred. PQI was found adding PW+PQS and RRI was defined with the difference between each R-peak. Each parameter variability in time was calculated using equation 1, where *par* is the parameter measured (e.g. QRS, PQI, and so on),  $VT_{par}$  is the parameter variability, *N* is the number of beats recorded (about 150 beats) and  $\overline{par}$  is the mean of the parameter in each ECG

trace taken in consideration. Variability in time is given in  $ms^2$ .

$$VT_{par} = \frac{1}{N} \sum_{i=1}^N (par_i - \overline{par})^2 \quad (1)$$

### B. Classification in Amplitude of Normal ECG Traces

The ECG trace physiological nature makes the process of identifying its ECG waveforms in amplitude a very complicated issue. The application of time-frequency analysis gives us an important alternative to study and to identify these ECG waveforms in amplitude. We defined amplitude parameters for X and Y leads in each ECG trace as the mean of ST interval amplitude (STIA), P wave amplitude (PWA), R-peak amplitude (RA), T wave amplitude (TWA) and Q wave amplitude (QWA). We applied a special treatment for Z lead that has different behavior, thus we defined three more parameters described as T wave with negative and positive in amplitude (NTWA and PTWA) and PQ amplitude (PQA) as shown in Fig. 5.

#### 1) Detection of critical points for X and Y leads

The wavelet transform is a very used technique for Time-Frequency Representations for ECG traces [8]. In this particular issue, we used the Continuous Wavelet Transform (CWT) as a tool to identify characteristic points in time amplitude and extract components localized in high and low frequencies of the signal ECG(t) for X and Y leads. The CWT is defined in equation 2.

$$CWT(b, a)_{ECG} = \frac{1}{\sqrt{a}} \int_{-\infty}^{+\infty} ECG(t) \Psi^* \left( \frac{t-b}{a} \right) dt \quad (2)$$

where the  $CWT(b, a)_{ECG}$  is the convolution of the ECG(t) trace and the conjugated wavelet function  $\Psi^*(t)$  that was shifted in time (*t*) by a parameter *b* and compressed in amplitude by a parameter *a*.

In order to identify different critical points that represent the beginning and ending of characteristic waves along all 36 ECG traces, we implemented the CWT by using MATLAB® with different scale (*H*) variations. An high scale was used for low frequency signals (e.g. T wave) and low scale was used for high frequency signals (e.g. QRS). Each critical point was determined by the time where  $\Psi(t)$  had a zero-crossing point. For signals that have Q and S waves we applied a scaled of  $H=2$ . The  $\Psi(t)$  higher peak was localized defining a dynamic threshold and a 50 ms temporal window around it. In order to detect the S wave higher peak, we moved this temporal window going forward and downward from the  $\Psi(t)$  higher peak to the zero-crossing point. In the same manner, to detect when the Q wave lower peak occurs, we moved this temporal window going backward and upward from the  $\Psi(t)$  lower peak to the  $\Psi(t)$  zero-crossing point. For QRS complex beginning (QRSON) and ending (QRSoFF) detection we used a  $\Psi(t)$  scaled in  $H=14$  and  $H=17$  respectively. QRSON was identified moving the temporal window again backward and upward from  $\Psi(t)$  lower peak to zero-crossing point. QRSoFF was localized moving the temporal window from  $\Psi(t)$  higher peak downward and forward to a  $\Psi(t)$  local minimum. Also applying  $H=20$  and  $H=17$  we identified P wave beginning and T wave ending respectively. We noticed that in  $\Psi(t)$  both waves have

almost the same behaviors but P wave occurs first than the T wave; thus we moved the temporal window from a  $\Psi(t)$  local minimum upward and backward to  $\Psi(t)$  zero-crossing point to find  $PW_{on}$ , and from  $\Psi(t)$  local maximum downward and forward to zero crossing point to find  $PW_{off}$ . Finally we moved the temporal window from a  $\Psi(t)$  local minimum backward and upward to  $\Psi(t)$  zero-crossing point in order to find  $TW_{on}$  and from a  $\Psi(t)$  local maximum downward and forward in order to find  $TW_{off}$ . Fig. 4 shows a complete description of  $\Psi(t)$  and  $ECG(t)$  relationship applying this temporal window for different scales in X and Y leads.

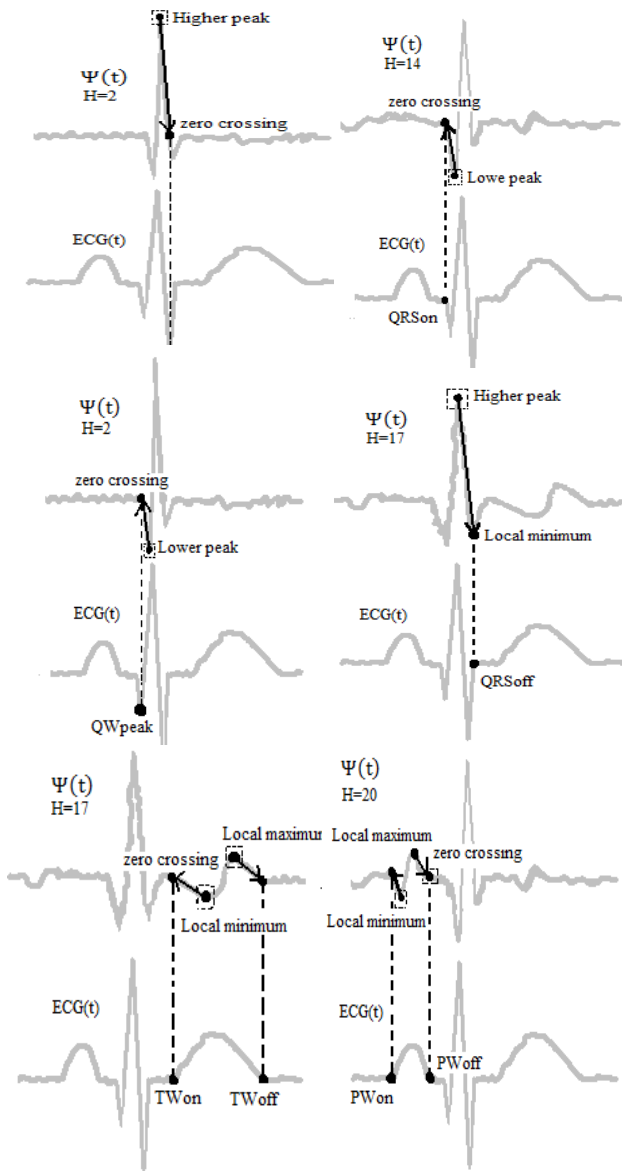


Fig. 4. Relationship between Wavelet transform with different scales and  $ECG(t)$ . Each critical point detected in  $ECG(t)$  were used as reference to find waveform amplitudes.

### 2) Detection of critical points for Z leads

The Frank Z lead is a very different ECG waveform in comparison with X and Y leads. In all Z lead traces we noticed that P and S waves were not presented. On the other hand, Z lead traces always presented a well-defined Q wave, a fact that not always happened with X and Y leads. Furthermore we noticed that T wave behavior is biphasic

with a falling slope in T wave beginning ( $TW_{on}$ ) followed by a rising slope for T wave ending ( $TW_{off}$ ). In order to extract information according to the waveform of the Z lead, we modified the algorithm to detect crucial points that better described it. Critical points that better defined the ECG waveforms in the X lead were compared with Z lead and they were used to define its own waveforms. Critical points where X and Z lead coincided were the Q wave peak ( $Q_{peak}$ ), R wave peak ( $R_{peak}$ ) and  $QRS_{off}$  as shown in Fig. 5.

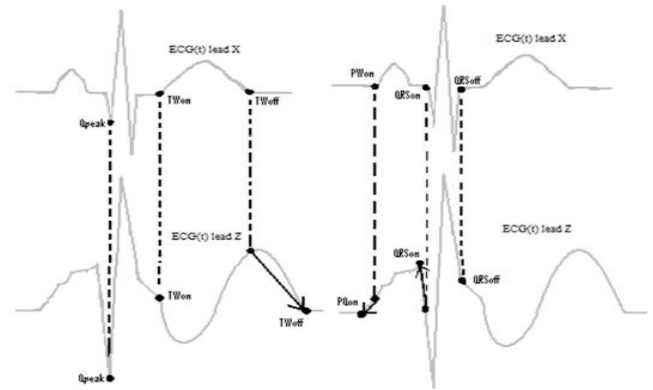


Fig. 5. The Z lead presented a biphasic T wave labeled as  $TW_{on}$  and  $TW_{off}$ , two parameters taken as critical points. The X lead parameters were used as reference to detect critical points in the Z lead.

We noticed that X lead  $TW_{on}$  and Z lead  $TW_{off}$  coincided, as well as X lead  $Q_{peak}$  coincided with Z lead  $Q_{peak}$  along all ECG traces, thus we defined  $Q_A$  and  $R_A$  for Z lead as the maximum negative and maximum positive detection respectively.

On the other hand, X lead  $TW_{off}$  did not coincide with Z lead  $TW_{off}$ . Thus we had to move this not coincidence point downward and forward until T wave stopped to decrease in order to find Z lead  $TW_{off}$ .  $NTW_A$  was defined as the maximum negative T wave and  $PTW_A$  as maximum positive T wave.

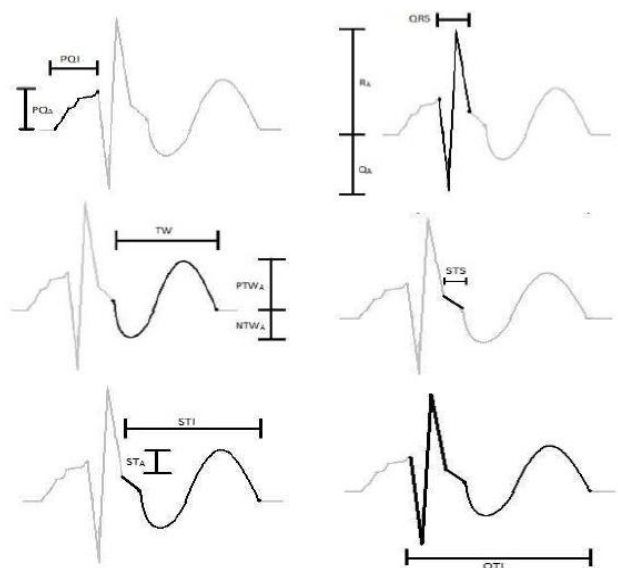


Fig. 6. Time and amplitude parameters taken in consideration to compute the ECG variability for Z lead.

We also noticed that X lead  $QRS_{off}$  coincided with Z lead  $QRS_{off}$ , thus we computed the Z lead ST segment ( $STS$ ) in time with the difference between  $TW_{on}$  minus  $QRS_{off}$ ; and  $ST$

segment in amplitude ( $ST_A$ ) as the maximum peak between them. Z lead  $Q_A$  generally has a very pronounced falling slope compared with other leads. The amplitude of PQ interval (PQI) was computed by the difference between  $QRS_{on}$  minus  $PQ_{on}$  and we labeled this parameter as  $PQ_A$ . A complete description of parameters taken in consideration for Z lead re show in Fig. 6.

Once all the ECG waveforms were defined, a simple maximum-peak detection algorithm was developed to find the maximum value for the P, R and T waves as the amplitude reference, with the exception of the  $STI_A$  that was measured from the difference between  $TW_A$  and  $QRS_{off}$ .

TABLE I: MAXIMUM VOLTAGES IN EACH ECG TRACE

Trace	Lead X max(mV)	Lead Y max(mV)	Lead Z max(mV)
104	2.54	1.01	1.03
116	1.44	0.70	0.84
117	1.79	1.45	1.12
150	1.78	1.83	0.63
155	1.35	0.85	1.00
156	0.73	2.68	1.66
165	1.70	0.70	0.88
166	4.67	1.43	1.09
169	1.17	0.63	0.82
170	1.84	0.39	0.98
172	1.66	0.82	1.17
173	0.99	1.26	0.83
174	1.46	1.09	0.91
180	1.04	0.47	0.74
182	1.69	0.94	0.50
214	1.08	0.84	1.27
234	1.04	1.01	0.64
235	1.50	0.28	1.14
237	1.42	0.70	0.71
238	1.09	0.70	1.04
239	0.86	0.34	1.17
240	0.95	1.03	1.22
241	2.39	1.48	1.40
242	0.90	1.54	1.45
243	0.87	1.13	0.32
244	1.71	0.59	0.65
245	1.38	0.66	0.94
251	1.04	0.59	1.16
252	2.12	0.61	0.78
255	1.04	0.99	1.46
260	0.92	1.29	1.29
264	1.62	0.92	0.71
267	1.22	0.55	0.93
276	1.52	0.70	1.01
277	1.94	0.99	0.61
284	1.21	1.71	1.03

Each parameter variability in amplitude was calculated using Equation 3, where  $par$  is the amplitude parameter measured (e.g. R, T, and so on),  $VA_{par}$  is the parameter variability,  $N$  is the number of beats recorded (about 150 beats) and  $\overline{par}$  is the mean of the parameter in amplitude for each ECG trace taken in consideration.

$$VA_{par} = \frac{1}{N} \sum_{i=1}^N (par_i - \overline{par})^2 \quad (3)$$

We established the maximum detected value as the reference in which all amplitude values should be normalized as we can see in Table I, thus if we have an amplitude value of one, this represents the maximum percentage (100%) and its Variability in amplitude is given in %<sup>2</sup>.

### III. RESULTS

In Appendix section we can see Table II(A) and Table II(B) continued for time-parameters and time-variability and in Table III and Table III continued for amplitude-parameters and amplitude-variability. All this tables and information are related with all ECG traces and leads taken from PTBDED. These tables have the mean and variability for each wave, segment, interval and complex. The mean and variability time parameters tables give the data of the duration in milliseconds of each parameter measured by the algorithms. As expected from healthy controls traces, the variability is very low, practically zero in some cases.

As we described before in algorithm implementation, all ECG traces were smoothed, adjusted to an isoelectric baseline and normalized to 1 as the highest value. All the amplitudes are presented in percentages and were measured from the baseline to the highest peak of each parameter. Some R wave peaks amplitude parameters are over 100% because the baseline is not in zero but lower. The percentages are equivalent to a voltage value in mV and these are presented in Table I for each trace and lead. Compared in time, the variability presented some changes through the ECG trace but did not cause a major change to the mean value. These findings tell us that the ECG variability trace are very low, even though between leads could present some significant differences in amplitude and time.

### IV. CONCLUSION

The old algorithms as the Pan-Tompkins are still a good QRS onset detection and the remaining characteristic waveforms of the ECG trace. Furthermore with these algorithms, the wavelet transform gives the advantage to work with no significance variations in amplitude due to it compares with a reference waveform called wavelet transform with different scales. This is a very useful technique because the ECG trace baseline is not stable and his waveforms identification were crucial. We implemented different algorithms for a complete database that contains the variability in time and amplitude of healthy ECG traces. We can see that there is almost no change in the waveforms, complexes and intervals within same lead but between different leads amplitude variability changes are consistent. This information is part of a greater project that pretends to get a mathematician model from healthy ECG traces.

APPENDIX

TABLE II(A): PARAMETERS AND VARIABILITY IN TIME OF X, Y AND Z LEADS (TRACES 104-244)

Trace/Par	STI(ms) ±V <sub>STI</sub> (ms <sup>2</sup> )	PQI(ms) ±V <sub>PQI</sub> (ms <sup>2</sup> )	PW(ms) ±V <sub>PW</sub> (ms <sup>2</sup> )	PQS(ms) ±V <sub>PQS</sub> (ms <sup>2</sup> )	QTI(ms) ±V <sub>QTI</sub> (ms <sup>2</sup> )	RRI(ms) ±V <sub>RRI</sub> (ms <sup>2</sup> )	QRS(ms) ±V <sub>QRS</sub> (ms <sup>2</sup> )	STS(ms) ±V <sub>STS</sub> (ms <sup>2</sup> )	TW(ms) ±V <sub>TW</sub> (ms <sup>2</sup> )
104	X:309±0.0076 Y: 286±0.008 Z: 426±0.008	X:142±0.14 Y: 162±0.14 Z:159±0.107	X:99.6±0.107 Y: 142±0.107 Z:ND	X:43.2±0.014 Y:20.2±0.014 Z:ND	X:391±0.013 Y:414±0.014 Z:542±0.017	X:969±4.11 Y:969±4.13 Z:969±4.12	X:82±0.006 Y:128±0.007 Z:115±0.007	X:125±0.015 Y:112±0.016 Z:125±0.015	X:185±0.022 Y:175±0.022 Z:302±0.022
116	X: 326 ±0.076 Y:316 ±0.008 Z: 416±0.008	X: 203 ±1.05 Y:203 ±1.05 Z: 198±1.06	X:130 ±0.006 Y:130 ±1.06 Z: ND	X: 73 ±0.006 Y:73 ±0.007 Z: ND	X:406±0.008 Y:406±0.008 Z: 00±0.012	X:972±0.67 Y:972±0.676 Z:972±0.672	X:80±0.0003 Y:89±0.0003 Z: 85±0.007	X:155 ±0.05 Y:144 ±0.05 Z:155±0.057	X:171 ±0.06 Y:171 ±0.063 Z:261±0.063
117	X: 274±0.002 Y: 273±0.002 Z: 353±0.002	X:183±0.007 Y:183±0.008 Z:211±0.006	X:117±0.006 Y:117±0.006 Z: ND	X: 66±0.0017 Y:66 ±0.002 Z: ND	X:369±0.002 Y:369±0.002 Z:480±0.005	X:874 ±1.54 Y:874±1.545 Z:874±1.607	X:95±0.0007 Y:95 ±0.001 Z:127±0.002	X: 70 ±0.013 Y:105±0.013 Z: 70±0.013	X:204±0.013 Y:169±0.014 Z:283±0.014
150	X:319 ±0.22 Y:319 ±0.22 Z: 420±0.220 X:285±0.0062 Y:277 ±0.006 Z: 285±0.006	X:166 ±0.22 Y: 165±0.22 Z:205±0.236 X:174±0.023 Y:196±0.023 Z:169±0.025	X:98 ±0.236 Y:98 ±0.236 Z: ND X:109±0.0123 Y:91 ±0.012 Z: ND	X:67 ±0.013 Y:67 ±0.013 Z: ND X:53 ±0.0016 Y:82 ±0.002 Z: ND	X:402±0.206 Y:402±0.207 Z:518±0.207 X:352±0.005 Y:365±0.006 Z:400±0.007	X:908±1.75 Y:907±1.77 Z:907±1.76 X:872 ±1.55 Y:772±1.542 Z: 771±1.55	X:908±1.75 Y:83±0.013 Z: 98±0.025 X:87±0.0004 Y:87±0.0004 Z:115±0.002	X:129±0.70 Y:129±0.701 Z:129±0.701 X:108±0.035 Y:108±0.035 Z: 98±0.035	X:190 ±0.17 Y:190 ±0.17 Z:291±0.172 X:176 ±0.02 Y:168 ±0.02 Z: 185±0.029
155	X:274±0.002 Y: 273±0.002 Z: 353±0.002	X:183±0.007 Y:183±0.008 Z:211±0.006	X:117±0.006 Y:117±0.006 Z: ND	X: 66±0.0017 Y:66 ±0.002 Z: ND	X:369±0.002 Y:369±0.002 Z:480±0.005	X:874 ±1.54 Y:874±1.545 Z:874±1.607	X:95±0.0007 Y:95 ±0.001 Z:127±0.002	X: 70 ±0.013 Y:105±0.013 Z: 70±0.013	X:204±0.013 Y:169±0.014 Z:283±0.014
156	X:310±0.002 Y:310 ±0.002 Z: 433±0.002 X:306±0.0023 Y:306 ±0.002 Z: 456±0.002	X:161±0.0049 Y: 161±0.005 Z: 224±0.005 X:167±0.013 Y: 206±0.014 Z: 205±0.014	X:116±0.0046 Y:116 ±0.005 Z: ND X:97±0.016 Y:135±0.017 Z: ND	X:45 ±0.0015 Y:45 ±0.002 Z: ND X:71 ±0.0028 Y:70±0.003 Z: ND	X:395±0.0021 Y:395±0.002 Z: 535±0.003 X:412±0.0020 Y:412±0.002 Z: 562±0.002	X:861 ±4.86 Y:861 ±4.668 Z: 861±4.62 X:1025±0.99 Y:1025±0.994 Z: 1024±0.99	X:88 ±0.017 Y:88 ±0.018 Z:107±0.007 X:85±0.0003 Y:85±0.0003 Z:101±0.001	X:74 ±0.05 Y:84 ±0.05 Z: 74±0.050 X:121±0.014 Y:120±0.014 Z:120±0.014	X:192 ±0.04 Y:174 ±0.04 Z: 287±0.046 X:189±0.014 Y:189±0.014 Z: 312±0.014
165	X:326 ±0.086 Y:326 ±0.087 Z: 456±0.087	X:135±0.1024 Y: 144±0.102 Z: 211 ±0.384	X:103±0.3843 Y:113±0.384 Z: ND	X:31 ±0.1040 Y:31 ±0.1040 Z: ND	X:408±0.0259 Y:409±0.026 Z: 552±0.037	X:1052±3.68 Y:1052±3.704 Z: 1052±3.69 X:636±0.239 Y:636 Z: 97±0.009	X:83±0.0731 Y:83 ±0.073 Z:96±0.146 X:97±0.0088 Y:97±0.009 Z: 97±0.009	X:143±0.123 Y:142±0.123 Z:142±0.123 X:72±0.0534 Y:72 ±0.053 Z: 72±0.053	X:183±0.059 Y:183±0.059 Z: 313±0.059 X:186±0.054 Y:166±0.054 Z: 243±0.054
170	X:258±0.0057 Y:238 ±0.006 Z: 315±0.006	X:118±0.1975 Y: 168±0.197 Z: 133±0.192	X:60 ±1.76 Y:116 ±1.761 Z: ND	X:58±1.38 Y:52 ±1.38 Z: ND	X:355±0.0151 Y:336 ±0.015 Z: 413±0.015	X:636±0.23 Y:889±0.5015 Z: 888±0.505	X:97±0.0088 Y:97±0.009 Z: 97±0.009	X:72±0.0534 Y:72 ±0.053 Z: 72±0.053	X:186±0.054 Y:166±0.054 Z: 243±0.054
172	X:314±0.0032 Y:343 ±0.003 Z: 393±0.003	X:155±0.0432 Y: 184±0.043 Z: 163±0.082	X:97±0.0824 Y:126±0.082 Z: ND	X:58±0.0547 Y:58±0.055 Z: ND	X:418±0.0088 Y:417 ±0.009 Z: 517±0.047	X:889±0.5015 Y:888±0.505 Z: 888±0.51	X:104±0.007 Y:74 ±0.007 Z:124±0.047	X:107±0.021 Y:136±0.021 Z:106±0.021	X:207±0.022 Y:206±0.022 Z: 286±0.022
173	X:316±0.0318 Y:315 ±0.032 Z: 410±0.032	X:163±0.0695 Y:173 ±0.069 Z: 158±0.065	X:108±0.0647 Y:117 ±0.065 Z: ND	X:55±0.0062 Y:55 ±0.006 Z: ND	X:391±0.0365 Y:390 ±0.036 Z: 503±0.027	X:909 ±20 Y:909 Z: 909±19.7	X:75±0.0011 Y:75 ±0.001 Z: 93±0.005	X:128±0.044 Y:128±0.044 Z:128±0.044	X:187±0.023 Y:187±0.023 Z: 282±0.023
174	X:298±0.0047 Y:318 ±0.005 Z: 407±0.005	X:186±0.0077 Y:192 ±0.008 Z: 192±0.005	X:95 ±0.0048 Y:101 ±0.005 Z: ND	X:91 ±0.0085 Y:91±0.009 Z: ND	X:403±0.0052 Y:402 ±0.005 Z: 524±0.017	X:916±0.6365 Y:916±0.676 Z: 915±0.63	X:104±0.0003 Y:84±0.0003 Z:117±0.008	X:101 ±0.02 Y:121 ±0.02 Z:101±0.021	X:197±0.013 Y:197±0.013 Z: 306±0.013
180	X:271±0.0755 Y:253±0.075 Z: 371±0.075	X:131 ±0.073 Y:150 ±0.073 Z: 123±0.088	X:77 ±0.0881 Y:96 ±0.088 Z: ND	X:54±0.0048 Y:54±0.005 Z: ND	X:362±0.0016 Y:362 ±0.002 Z: 516±0.005	X:888 ±1.78 Y:888 ±1.76 Z: 888±1.79	X:91±0.077 Y:110±0.077 Z:145±0.081	X:92±0.103 Y:99 ±0.103 Z: 91±0.103	X:179±0.039 Y:153±0.039 Z: 279±0.039
182	X:296±0.0018 Y:296 ±0.002 Z: 396±0.002	X:186±0.0053 Y:178 ±0.005 Z: 170±0.005	X:115±0.0055 Y:104 ±0.005 Z: ND	X:71 ±0.0021 Y:74 ±0.002 Z: ND	X:373 ±0.002 Y:379 ±0.002 Z: 487±0.003	X:839±0.7557 Y:839 Z: 839±0.76	X:76±0.0003 Y:83±0.0003 Z: 91±0.002	X:95±0.021 Y:124±0.021 Z: 94±0.021	X:201 ±0.02 Y:171±0.022 Z: 301±0.022
214	X:241±0.0014 Y:240 ±0.001 Z: 273±0.001	X:148±0.0165 Y:143 ±0.016 Z: 124±2.70	X:62 ±2.7 Y:75 ±2.7 Z: ND	X:86 ±2.73 Y:67 ±2.73 Z: ND	X:322±0.0014 Y:341 ±0.001 Z: 401 ±2.732	X:611 ±0.3992 Y:611 Z: 611±0.4	X:81±0.0005 Y:100±0.0005 Z: 127±2.73	X:77±0.0346 Y:77 ±0.035 Z: 77±0.035	X:164±0.035 Y:163±0.035 Z: 196±0.035
234	X:329±0.0472 Y:343 ±0.009 Z: 499±0.009	X:208±0.0652 Y:203 ±0.065 Z: 248±0.074	X:109±0.0741 Y:108 ±0.074 Z: ND	X:100±0.0076 Y:95 ±0.008 Z: ND	X:437±0.0092 Y:441 ±0.009 Z: 619±0.013	X:113 Y:113±4.858 Z: 1113±4.85	X:107±0.0004 Y:99±0.0004 Z:120±0.007	X:138±0.016 Y:152±0.016 Z:138±0.016	X:191±0.008 Y:190±0.009 Z: 360±0.009
235	X:301±0.0096 Y:287 ±0.010 Z: 391±0.010	X:175 ±0.017 Y:175 ±0.018 Z: 153±0.025	X:125±0.0246 Y:125 ±0.025 Z: ND	X:50 ±0.0061 Y:50 ±0.006 Z: ND	X:387±0.011 Y:387 ±0.011 Z: 528±0.013	X:890 ±6.12 Y:890 ±6.22 Z: 890±6.12	X:86±0.0003 Y:99±0.0003 Z:136±0.005	X:98 ±0.03 Y:139±0.034 Z:135±0.034	X:202±0.401 Y:148 ±0.04 Z: 256±0.040
237	X:296±0.0016 Y:287 ±0.002 Z: 422±0.002	X:165±0.0122 Y:164 ±0.012 Z: 152±0.007	X:111±0.0071 Y:111 ±0.007 Z: ND	X:53 ±0.0069 Y:53 ±0.007 Z: ND	X:388±0.0019 Y:388 ±0.002 Z: 526±0.008	X:981 ±0.3809 Y:981 Z: 981±0.38	X:91±0.0004 Y:100±0.0004 Z:103±0.006	X:103±0.013 Y:112±0.014 Z:103±0.014	X:193±0.014 Y:176±0.015 Z: 319±0.015
238	X:287±0.0088 Y:273 ±0.009 Z: 363±0.009	X:140 ±0.009 Y:140±0.009 Z:112±0.012	X:112 ±0.012 Y: 112±0.012 Z: ND	X:29±0.0036 Y:29±0.004 Z: ND	X:372±0.0097 Y:372±0.010 Z: 477±0.007	X:764 ±4.07 Y:765 ±4.10 Z:764±4.09	X:85±0.0004 Y:98±0.0004 Z:113±0.003	X:103±0.043 Y:140±0.043 Z:102±0.043	X:183±0.043 Y:133±0.043 Z: 260±0.043
239	X:319±0.0256 Y:311 ±0.026 Z: 319±0.026	X:139 ±1.02 Y:152 ±1.026 Z: 142±1.11	X:113 ±1.11 Y:125 ±1.18 Z: ND	X:26 ±0.02 Y:27 ±0.02 Z: ND	X:388 ±0.027 Y:388 ±0.028 Z: 414±0.036	X:745 ±8.85 Y:745 ±8.83 Z: 745±8.83	X:69±0.0014 Y:76 ±0.001 Z: 95±0.017	X:143±0.379 Y:136±0.379 Z:115±0.379	X:175±0.352 Y:175±0.353 Z: 203±0.35
240	X:292 ±0.009 Y:291 ±0.009 Z: 390±0.009	X:149±0.0209 Y:165 ±0.021 Z: 152±0.022	X:100±0.0217 Y:117 ±0.022 Z: ND	X:49 ±0.0047 Y:49 ±0.005 Z: ND	X:368±0.0101 Y: 368±0.010 Z: 490±0.018	±0.603 Y:771 Z: 605	X:76±0.0003 Y:76±0.0003 Z: 99±0.005	X:104±0.065 Y:113±0.066 Z:104±0.066	X:188±0.074 Y:177±0.075 Z: 286±0.075
241	X:315±0.0046 Y:315 ±0.005 Z: 391±0.005	X:156±0.0416 Y:148 ±0.042 Z: 147±0.041	X:86 ±0.0407 Y:86 ±0.041 Z: ND	X:71 ±0.0021 Y:63 ±0.002 Z: ND	X:400±0.0051 Y:408 ±0.005 Z: 484±0.007	X:1077 ±5.6 Y:1077±5.619 Z: 1077±5.63	X:85±0.0004 Y:93±0.0004 Z: 93±0.002	X:118±0.013 Y:118±0.013 Z:117±0.013	X:197±0.014 Y:197±0.015 Z: 273±0.015
242	X:273±0.0023 Y:272 ±0.002 Z: 333±0.002	X:150±0.0197 Y:153 ±0.02 Z: 138±0.021	X:93 ±0.0211 Y:123 ±0.021 Z: ND	X:56±0.0092 Y:30±0.009 Z: ND	X:357±0.0049 Y:383 ±0.005 Z: 474±0.008	X:831 ±1.74 Y:831 ±1.74 Z:831 ±1.74	X:85±0.0026 Y:111±0.003 Z:141±0.007	X:90±0.0434 Y:90 ±0.043 Z:159±0.043	X:183±0.042 Y:183±0.043 Z: 173±0.043
243	X:254 ±0.006 Y:254 ±0.006 Z: 253±0.006	X:150 ±2.47 Y:172 ±2.47 Z: 147±3.27	X:90 ±3.26 Y:131 ±3.27 Z: ND	X:60 ±1.23 Y:41 ±1.231 Z: ND	X:340±0.0064 Y:345 ±0.006 Z: 379±1.18	X:651±0.7986 Y:651±0.801 Z: 651±0.81	X:86±0.0005 Y:91±0.0005 Z:125±1.235	X:69±0.0815 Y:80 ±0.081 Z: 69±0.081	X:185±0.091 Y:173±0.09 Z: 184±0.091

244	X:262 ±0.034 Y:262 ±0.034 Z: 338 ±0.034	X:159 ±0.014 Y:158 ±0.014 Z: 152 ±0.012	X:105 ±0.012 Y:104 ±0.012 Z: ND	X:53 ±0.0072 Y:54 ±0.007 Z: ND	X:367 ±0.0011 Y:367 ±0.001 Z: 451 ±0.007	X:803 ±0.18 Y:803 ±0.185 Z: 831 ±0.17	X:106 ±0.035 Y:106 ±0.035 Z:113 ±0.040	X:99 ±0.0437 Y:99 ±0.044 Z: 98 ±0.044	X:163 ±0.016 Y:163 ±0.017 Z: 240 ±0.017
-----	---	---	---------------------------------------	--------------------------------------	--	--	--	---	---

TABLE II(B): PARAMETERS AND VARIABILITY IN TIME OF X, Y AND Z LEADS (TRACES 245-284)

Trace/ Par	PW <sub>A</sub> (%) ±VPW <sub>A</sub> (%) <sup>2</sup>	RA(%) ±VRA(%) <sup>2</sup>	STA(%) ±VSTA(%) <sup>2</sup>	TWA(%) ±VTWA(%) <sup>2</sup>	PQIA(%) ±PQIA(%) <sup>2</sup>	QA(%) ±QA(%) <sup>2</sup>	PTWA(%) ±PTWV(%) <sup>2</sup>	NTWA(%) ±NTWV(%) <sup>2</sup>
104	X: 3.08 ±0.0007 Y:16.51 ±0.0205 Z: ND	X: 95.45 ±0.1628 Y: 96.36 ±0.1628 Z: 100.51 ±0.0423	X:14.02 ±0.0127 Y:24.53 ±0.0362 Z: 3.06 ±0.1418	X:14.90 ±0.0127 Y:26.15 ±0.0328 Z:ND	X: ND Y: ND Z:5.72 ±0.0309	X: ND Y: ND Z: -13.90 ±0.04	X: ND Y: ND Z: 12.28 ±0.094	X:ND Y:ND Z:-4.51 ±0.047
116	X: 9.97 ±0.0205 Y: 9.07 ±0.0580 Z: ND	X: 98.99 ±0.1132 Y: 89.78 ±0.3416 Z: 98.16 ±0.1961	X: 7.59 ±0.1186 Y: 0.35 ±0.2756 Z: -10.25 ±0.270	X:14.01 ±0.0109 Y:12.24 ±0.0254 Z:ND	X: ND Y: ND Z:10.72 ±0.177	X: ND Y: ND Z: -31.10 ±0.11	X: ND Y: ND Z: 3.01 ±0.015	X:ND Y:ND Z:-2.38 ±0.009
117	X: 5.51 ±0.0088 Y: 6.01 ±0.0086 Z: ND	X: 98.73 ±0.0623 Y: 99.11 ±0.0762 Z: 87.43 ±0.4551	X:16.04 ±0.0644 Y: 5.89 ±0.1322 Z: -8.55 ±0.3059	X:20.42 ±0.0104 Y:12.60 ±0.0101 Z:ND	X: ND Y: ND Z:28.04 ±0.531	X: ND Y: ND Z: -18.73 ±0.32	X: ND Y: ND Z:10.55 ±0.150	X:ND Y:ND Z:-3.49 ±0.088
150	X: 5.96 ±0.0019 Y: 2.14 ±0.0036 Z: ND	X: 103.55 ±0.0193 Y: 99.05 ±0.0954 Z: 53.10 ±0.3611	X:24.25 ±0.0931 Y:13.01 ±0.7539 Z: 2.35 ±1.6963	X:29.88 ±0.0399 Y:17.38 ±0.5205 Z:ND	X: ND Y: ND Z:11.14 ±0.459	X: ND Y: ND Z:-15.81 ±0.25	X: ND Y: ND Z:11.92 ±0.613	X: ND Y: ND Z: -7.81 ±0.893
155	X:11.58 ±0.3085 Y:14.76 ±0.0087 Z: ND	X: 90.40 ±0.4221 Y: 98.39 ±0.0869 Z: 95.24 ±0.1922	X: -0.36 ±0.4659 Y:10.04 ±0.0516 Z: 3.15 ±0.0086	X:16.28 ±0.1574 Y:13.80 ±0.0271 Z:ND	X: ND Y: ND Z:1.25 ±0.006	X: ND Y: ND Z: -9.64 ±0.008	X: ND Y: ND Z: 3.18 ±0.002	X: ND Y: ND Z: -2.38 ±0.010
156	X:14.51 ±0.0820 Y: 5.50 ±0.0024 Z: ND	X: 101.54 ±0.1994 Y: 101.90 ±0.0351 Z: 98.70 ±0.2330	X:63.99 ±0.6541 Y:20.50 ±0.0542 Z: -2.74 ±0.1912	X:71.22 ±0.3611 Y:24.33 ±0.0079 Z:ND	X: ND Y: ND Z:13.19 ±0.136	X: ND Y: ND Z:-14.78 ±1.26	X: ND Y: ND Z: 9.28 ±0.075	X: ND Y: ND Z: -3.98 ±0.080
165	X: 5.47 ±0.0004 Y: 8.73 ±0.0141 Z: ND	X: 102.37 ±0.0598 Y: 100.94 ±0.0620 Z: 100.68 ±0.0923	X:30.62 ±0.0735 Y:13.27 ±0.1874 Z: 16.10 ±1.2091	X:34.34 ±0.0124 Y:18.99 ±0.0497 Z:ND	X: ND Y: ND Z:23.41 ±0.221	X: ND Y: ND Z: -45.66 ±0.18	X: ND Y: ND Z:39.74 ±1.352	X: ND Y: ND Z: -9.68 ±0.381
166	X: 3.60 ±0.026 Y:10.58 ±0.0057 Z: ND	X: 101.93 ±0.1035 Y: 94.36 ±0.3758 Z: 90.14 ±1.1995	X:15.35 ±0.1328 Y:21.58 ±0.1139 Z: -12.30 ±0.750	X:23.15 ±0.0193 Y:25.23 ±0.0338 Z:ND	X: ND Y: ND Z:31.26 ±0.457	X: ND Y: ND Z: -20.68 ±0.24	X: ND Y: ND Z:11.08 ±0.107	X: ND Y: ND Z: -4.13 ±0.031
169	X: 5.08 ±0.0033 Y:17.72 ±0.0569 Z: ND	X: 98.97 ±0.0364 Y: 96.93 ±0.1697 Z: 99.81 ±0.1062	X:24.09 ±0.0156 Y:14.22 ±0.1177 Z: -6.66 ±0.173	X:23.58 ±0.0090 Y:20.05 ±0.0310 Z:ND	X: ND Y: ND Z:11.63 ±0.073	X: ND Y: ND Z: -22.29 ±0.06	X: ND Y: ND Z: 7.39 ±0.034	X: ND Y: ND Z: -3.04 ±0.027
170	X: 7.13 ±0.4786 Y:44.25 ±0.2234 Z: ND	X: 99.58 ±0.2732 Y: 94.22 ±0.7130 Z: 101.58 ±0.3931	X: 6.22 ±0.3233 Y:46.38 ±0.2683 Z: -3.13 ±0.2130	X:20.90 ±0.1626 Y:42.84 ±0.1309 Z:ND	X: ND Y: ND Z:11.07 ±0.442	X: ND Y: ND Z: -39.72 ±1.02	X: ND Y: ND Z: 10.02 ±0.119	X: ND Y: ND Z: -8.62 ±0.262

TABLE III(A): PARAMETERS AND VARIABILITY IN AMPLITUDE OF X, Y AND Z LEADS (TRACES 104-170)

Trace /Par	STI(ms) ±VSTI(ms <sup>2</sup> )	PQI(ms) ±VPQI(ms <sup>2</sup> )	PW(ms) ±VPW(ms <sup>2</sup> )	PQS(ms) ±VPQS(ms <sup>2</sup> )	QTI(ms) ±VQTI(ms <sup>2</sup> )	RRI(ms) ±VRRI(ms <sup>2</sup> )	QRS(ms) ±VQRS(ms <sup>2</sup> )	STS(ms) ±VSTS(ms <sup>2</sup> )	TW(ms) ±VTW(ms <sup>2</sup> )
245	X:302 ±0.006 Y:301 ±0.006 Z:380 ±0.006	X:179 ±0.103 Y:168 ±0.103 Z: 149 ±0.131	X:122 ±0.131 Y:114 ±0.131 Z: ND	X:57 ±0.0284 Y:55 ±0.028 Z: ND	X:385 ±0.009 Y:395 ±0.009 Z: 493 ±0.024	X:980 ±13.6 Y:980 ±13.70 Z:980 ±13.4	X:83 ±0.0025 Y:93 ±0.003 Z: 113 ±0.026	X:116 ±0.071 Y:116 ±0.071 Z:115 ±0.071	X:186 ±0.077 Y:186 ±0.078 Z:265 ±0.078
251	X:302 ±0.0073 Y:272 ±0.007 Z: 392 ±0.007 X:333 ±0.0067	X:183 ±0.052 Y: 183 ±0.052 Z: 167 ±0.032 X:152 ±0.048	X:131 ±0.032 Y:114 ±0.032 Z: ND X:80 ±0.0469	X:51 ±0.0143 Y:68 ±0.014 Z: ND X:73 ±0.0027	X:379 ±0.008 Y:362 ±0.008 Z: 485 ±0.027 X:412 ±0.005	X:774 ±1.088 Y:774 ±1.089 Z: 774 ±1.08 X:981 ±1.93	X:77 ±0.0010 Y:90 ±0.001 Z: 93 ±0.016 X:78 ±0.0038	X:125 ±0.049 Y:112 ±0.049 Z:112 ±0.049 X:160 ±0.029	X:176 ±0.056 Y:160 ±0.056 Z:279 ±0.056 X:173 ±0.03
252	Y:333 ±0.007 Z:501 ±0.007 X:310 ±0.0361	Y:160 ±0.048 Z: 197 ±0.047 X:173 ±0.075	Y:97 ±0.047 Z: ND X:102 ±0.067	Y:62 ±0.003 Z: ND X:71 ±0.0679	Y: 412 ±0.005 Z: 597 ±0.005 X:415 ±0.052	Y:981 ±1.935 Z:981 ±1.93 X:916 ±0.588	Y:78 ±0.004 Z: 95 ±0.007 X:105 ±0.016	Y:160 ±0.03 Z:140 ±0.030 X:81 ±0.1626	Y:174 ±0.03 Z:361 ±0.030 X:229 ±0.177
255	Y:290 ±0.036 Z: 430 ±0.036 X:283 ±0.0049	Y:191 ±0.075 Z:190 ±0.068 X:129 ±0.030	Y: 120 ±0.068 Z: ND X: 97 ±0.0348	Y:71 ±0.019 Z: ND X:32 ±0.0348	Y:396 ±0.053 Z:542 ±0.046 X:365 ±0.005	Y:916 ±0.591 Z: 916 ±0.58 X:978 ±3.67	Y:105 ±0.016 Z: 112 ±0.006 X:81 ±0.0008	Y:89 ±0.163 Z: 81 ±0.163 X:99 ±0.0605	Y:201 ±0.178 Z:349 ±0.178 X:184 ±0.057
260	Y:283 ±0.005 Z:363 ±0.005 X:319 ±0.0027	Y:129 ±0.031 Z:122 ±0.035 X:161 ±0.215	Y:97 ±0.035 Z: ND X:103 ±0.238	Y:32 ±0.005 Z: ND X:58 ±0.2385	Y:365 ±0.005 Z:477 ±0.008 X:413 ±0.003	Y:978 ±3.690 Z: 978 ±3.69 X:963 ±2.47	Y:81 ±0.001 Z:113 ±0.003 X:94 ±0.0003	Y:99 ±0.06 Z: 99 ±0.061 X:123 ±0.017	Y:184 ±0.057 Z:264 ±0.057 X:195 ±0.02
264	Y:319 ±0.003 Z: 470 ±0.003 X:366 ±0.0014	Y:161 ±0.216 Z:171 ±0.238 X:179 ±0.011	Y:103 ±0.238 Z: ND X:123 ±0.009	Y:58 ±0.007 Z: ND X:55 ±0.0017	Y:413 ±0.003 Z: 587 ±0.009 X:453 ±0.001	Y:963 ±2.47 Z: 963 ±2.42 X:1091 ±0.88	Y:94 ±0.0003 Z:117 ±0.007 X:86 ±0.0003	Y:124 ±0.018 Z:123 ±0.018 X:170 ±0.013	Y:195 ±0.02 Z:346 ±0.020 X:170 ±0.014
267	Y:366 ±0.001 Z: 498 ±0.001 X:291 ±0.0055	Y:179 ±0.012 Z:166 ±0.010 X:129 ±0.067	Y:123 ±0.01 Z: ND X:67 ±0.0664	Y:55 ±0.002 Z: ND X:62 ±0.0025	Y:453 ±0.002 Z:598 ±0.004 X:378 ±0.005	Y:1091 ±0.89 Z: 1091 ±0.87 X:786 ±0.495	Y:86 ±0.0003 Z:100 ±0.002 X:87 ±0.0003	Y:170 ±0.013 Z:170 ±0.013 X:104 ±0.045	Y:196 ±0.014 Z:328 ±0.014 X:186 ±0.048
276	Y:271 ±0.006 Z:349 ±0.006 X:352 ±0.0029	Y:173 ±0.067 Z:156 ±0.066 X:149 ±0.011	Y:107 ±0.066 Z: ND X:83 ±0.0109	Y:66 ±0.003 Z: ND X:66 ±0.0028	Y:368 ±0.006 Z: 454 ±0.008 X:438 ±0.002	Y:786 ±0.494 Z: 786 ±0.49 X:1217 ±4.75	Y:96 ±0.0003 Z:105 ±0.002 X:86 ±0.0003	Y:84 ±0.046 Z:163 ±0.046 X:143 ±0.021	Y:186 ±0.048 Z:185 ±0.048 X:208 ±0.017
277	Y:352 ±0.003 Z:477 ±0.003 X:274 ±0.0038	Y:169 ±0.011 Z:114 ±0.011 X:166 ±0.044	Y:116 ±0.011 Z: ND X:90 ±0.1693	Y:53 ±0.003 Z: ND X:75 ±0.1515	Y:438 ±0.003 Z:629 ±0.005 X:361 ±0.004	Y:1217 ±4.76 Z:1217 ±4.8 X:795 ±1.79	Y:86 ±0.0003 Z:152 ±0.003 X:86 ±0.0003	Y:143 ±0.021 Z:143 ±0.021 X:92 ±0.047	Y:208 ±0.018 Z:333 ±0.018 X:182 ±0.047
284	Y:274 ±0.004 Z:424 ±0.004	Y:176 ±0.044 Z:171 ±0.169	Y:100 ±0.169 Z: ND	Y:76 ±0.152 Z: ND	Y:361 ±0.004 Z:523 ±0.154	Y:795 ±1.8 Z:795 ±1.82	Y:86 ±0.0003 Z:99 ±0.148	Y:102 ±0.047 Z: 92 ±0.047	Y:172 ±0.047 Z: 332 ±0.04

TABLE III(B): PARAMETERS AND VARIABILITY IN AMPLITUDE OF X, Y AND Z LEADS (TRACES 172-284)

Trace/ Par	PWA(%) ±VPWA(%) <sup>2</sup>	RA(%) ±VRA(%) <sup>2</sup>	STA(%) ±VSTA(%) <sup>2</sup>	TWA(%) ±VTWA(%) <sup>2</sup>	PQIA(%) ±PQIA(%) <sup>2</sup>	QA(%) ±QA(%) <sup>2</sup>	PTWA(%) ±PTWV(%) <sup>2</sup>	NTWA(%) ±NTWV(%) <sup>2</sup>
172	X:10.30 ±0.2747 Y:13.03 ±0.0136 Z: ND	X: 94.50 ±0.5025 Y: 93.91 ±0.2682 Z: 98.85 ±0.1927	X:12.56 ±0.2881 Y:13.22 ±0.0523 Z: 7.60 ±0.1266	X:24.75 ±0.0153 Y:22.25 ±0.0463 Z:ND	X: ND Y: ND Z:1.89 ±0.120	X: ND Y: ND Z: -7.96 ±0.19	X: ND Y: ND Z: 12.43 ±0.067	X: ND Y: ND Z: -6.36 ±0.123
173	X: 9.85 ±0.0125 Y:11.85 ±0.02 Z: ND	X: 95.37 ±0.4351 Y: 101.45 ±0.0307 Z: 97.39 ±0.1093	X:35.80 ±0.0983 Y:19.06 ±0.0195 Z: -0.76 ±0.0780	X:40.44 ±0.0584 Y:24.70 ±0.0088 Z:ND	X: ND Y: ND Z:6.81 ±0.0179	X: ND Y: ND Z:-22.2 ±0.02	X: ND Y: ND Z: 8.34 ±0.0506	X: ND Y: ND Z:-3.58 ±0.038
174	X: 5.36 ±0.4786	X: 99.68 ±0.0723	X:31.65 ±0.3603	X:43.16 ±0.0380	X: ND	X: ND	X: ND	X: ND

	Y:10.15±0.0142 Z: ND	Y: 102.61±0.0486 Z: 97.62±0.0630	Y:26.58±0.0663 Z: -0.82±0.1294	Y:35.51±0.0187 Z:ND	Y: ND Z: 8.98±0.0615	Y: ND Z:-12.6±0.04	Y: ND Z: 7.56±0.0162	Y: ND Z:-3±0.0279
180	X: 7.52±0.0033 Y:23.09±0.0478 Z: ND	X:99.97±0.072 Y: 99.73±0.2411 Z: 98.62±0.4943	X:28.59±0.1284 Y:41.74±0.4020 Z: 0.08±1.3535	X:37.59±0.0252 Y:54.66±0.1389 Z:ND	X:ND Y: ND Z:21.03±0.533	X: ND Y: ND Z:-69.8±0.47	X: ND Y: ND Z: 29.56±0.408	X: ND Y: ND Z:-11.74±0.62
182	X: 8.19±0.0029 Y:18.27±0.0067 Z: ND	X: 101.48±0.1217 Y: 100.92±0.0710 Z: 96.24±0.1590	X:23.50±0.0637 Y: 7.57±0.1230 Z: 7.56±0.6691	X:25.88±0.0176 Y:15.38±0.0158 Z:ND	X:ND Y: ND Z:14.61±0.117	X: ND Y: ND Z: -59.4±0.12	X: ND Y: ND Z: 21.50±0.252	X: ND Y: ND Z:-9.27±0.273
214	X: 8.93±0.3972 Y:19.06±0.0652 Z: ND	X: 103.95±0.3091 Y: 100.18±0.1904 Z: 98.20±0.1937	X:26.42±0.5086 Y:19.05±0.0779 Z: 6.02±0.6264	X:42.82±0.2165 Y:23.65±0.0289 Z:ND	X:ND Y: ND Z:4.37±0.1216	X: ND Y: ND Z:-16.6±0.10	X: ND Y: ND Z: 18.74±0.362	X: ND Y: ND Z:-9.54±0.294
234	X: 6.29±0.0209 Y:10.05±0.0285 Z: ND	X: 102.78±0.1304 Y: 102.24±0.0447 Z: 85.64±0.2776	X:34.76±0.3901 Y:19.73±0.0393 Z:10.27±0.1675	X:45.78±0.0423 Y:26.70±0.0210 Z:ND	X:ND Y: ND Z:6.79±0.0239	X: ND Y: ND Z:-14.1±0.04	X: ND Y: ND Z: 16.50±0.284	X: ND Y: ND Z:-5.9±0.009
235	X:10.13±0.0602 Y:59.76±0.4143 Z: ND	X: 98.58±0.1758 Y:99.30±0.13805 Z: 98.91±0.3104	X:18.27±0.0951 Y:37.91±0.0350 Z: -3.10±0.5911	X:23.91±0.0152 Y:57.72±0.3911 Z:ND	X:ND Y: ND Z:14.59±0.339	X: ND Y: ND Z:-29.5±0.22	X: ND Y: ND Z:12.91±0.1632	X: ND Y: ND Z:-6.73±0.051
237	X: 7.33±0.0011 Y: 6.85±0.0445 Z: ND	X: 103.40±0.0251 Y: 96.16±0.2035 Z: 103.21±0.1443	X:33.90±0.0710 Y:19.65±0.5585 Z:20.95±0.4566	X:35.97±0.0176 Y:35.32±0.0633 Z:ND	X:ND Y: ND Z:5.18±0.0141	X: ND Y: ND Z:-1.64±0.02	X: ND Y: ND Z:38.91±0.7833	X: ND Y: ND Z:-7.99±0.054
238	X:77.32±0.0011 Y:15.41±0.1498 Z: ND	X: 100.20±0.0724 Y: 89.88±0.8704 Z: 96.19±0.4490	X:12.80±0.0358 Y:-1.04±0.4450 Z: -8.99±0.2498	X:16.10±0.0137 Y:17.82±0.1186 Z:ND	X:ND Y: ND Z:10.93±0.155	X: ND Y: ND Z:-32.5±0.32	X: ND Y: ND Z: 4.25±0.1667	X: ND Y: ND Z:-6.87±0.278
239	X:9.85±0.0187 Y:52.70±0.6438 Z: ND	X: 98.44±0.3115 Y: 84.17±2.8349 Z: 98.56±0.049	X:-2.06±0.3138 Y:27.12±0.3317 Z: -6.53±0.092	X:15.76±0.0282 Y:34.56±0.3068 Z:ND	X:ND Y: ND Z:5.82±0.062	X: ND Y: ND Z:-25.1±0.08	X: ND Y: ND Z: 4.99±0.072	X: ND Y: ND Z:-4±0.034
240	X:8.16±0.0004 Y:11.05±0.0098 Z: ND	X: 97.85±0.1235 Y: 100.75±0.0423 Z: 98.24±0.3426	X:17.35±0.0598 Y:11.70±0.0121 Z: -2.40±0.2840	X:24.59±0.0209 Y:13.81±0.0092 Z:ND	X:ND Y: ND Z:12.71±0.193	X: ND Y: ND Z:-42.8±0.23	X: ND Y: ND Z: 8.90±0.0590	X: ND Y: ND Z:-7.73±0.164
241	X:3.33±0.0015 Y:7.28±0.0034 Z: ND	X: 100.88±0.0730 Y: 101.68±0.0250 Z: 97.09±0.1658	X:15.85±0.0582 Y: 1.30±0.0285 Z: -8±0.1924	X:22.61±0.0057 Y:14.94±0.0053 Z:ND	X:ND Y: ND Z:9.82±0.0523	X: ND Y: ND Z:-22.4±0.05	X: ND Y: ND Z:12.06±0.0685	X: ND Y: ND Z:-5.16±0.072
242	X:20.34±0.5847 Y:7.09±0.0169 Z: ND	X: 98.52±0.0730 Y: 100.54±0.0929 Z: 95.46±0.3248	X:16.11±1.4475 Y:14.25±0.0595 Z: -4.59±0.2055	X:47.62±0.1339 Y:20.44±0.0269 Z:ND	X:ND Y: ND Z:9.07±0.0955	X: ND Y: ND Z:15.4±0.75	X: ND Y: ND Z:-0.89±0.0415	X: ND Y: ND Z:-4.36±0.050
243	X:5.54±0.0232 Y:16.14±0.0629 Z: ND	X: 105.08±0.0555 Y: 104.26±0.0641 Z: 92.62±0.6850	X:31.23±0.0580 Y:18.11±0.0270 Z: -3.30±0.4061	X:34.61±0.0316 Y:19.53±0.0126 Z:ND	X:ND Y: ND Z:11.79±0.646	X: ND Y: ND Z:-39.9±0.49	X: ND Y: ND Z: 1.72±0.2504	X: ND Y: ND Z:-11.28±0.23
244	X:6.89±0.0068 Y:15.93±0.0226 Z: ND	X: 101.27±0.1450 Y: 100.20±0.2310 Z: 97.88±2.0105	X:27.59±0.1257 Y:42.87±0.1160 Z:-12.46±3.184	X:31.36±0.0103 Y:45.91±0.0538 Z:ND	X:ND Y: ND Z:43.64±2.887	X: ND Y: ND Z:-50.23±2.1	X: ND Y: ND Z:44.21±1.1510	X: ND Y: ND Z:-17.79±1.86
245	X:7.39±0.0080 Y:7.12±0.1464 Z: ND	X: 101.68±0.0613 Y: 90.18±0.6750 Z: 97.98±0.1907	X:23.92±0.1167 Y:4.54±0.1190 Z: 6±0.1316	X:29.11±0.0344 Y:13.41±0.0495 Z:ND	X:ND Y: ND Z:5.55±0.0218	X: ND Y: ND Z:-12.4±0.03	X: ND Y: ND Z:13.12±0.1575	X: ND Y: ND Z:-5.16±0.022
251	X:8.88±0.0143 Y:19.99±0.0519 Z: ND	X: 101.67±0.0914 Y: 98.01±0.1564 Z: 100.58±0.1234	X:23.84±0.0443 Y:22.75±0.0641 Z: -3.63±0.223	X:26.92±0.0150 Y:25.24±0.0372 Z:ND	X:ND Y: ND Z:8.10±0.0767	X: ND Y: ND Z:-22.03±0.1	X: ND Y: ND Z:13.04±0.0803	X: ND Y: ND Z:-5.32±0.051
252	X:3.01±0.0014 Y:11.65±0.0164 Z: ND	X: 100.16±0.0602 Y: 96.08±0.1317 Z: 99.65±0.2957	X:21.66±0.0249 Y:25.19±0.0484 Z:12.35±0.3551	X:25.75±0.0082 Y:30.91±0.0231 Z:ND	X:ND Y: ND Z:12.78±0.173	X: ND Y: ND Z:-31.4±0.13	X: ND Y: ND Z:32.39±0.3351	X: ND Y: ND Z:-9.69±0.066
255	X:5.94±0.0114 Y:12.08±0.0041 Z: ND	X: 99.73±0.1167 Y: 100.82±0.0410 Z: 103.13±0.0975	X:6.07±0.1294 Y:11.63±0.0060 Z: 3.15±0.1916	X:12.14±0.0580 Y:12.08±0.0091 Z:ND	X:ND Y: ND Z:9.78±0.1432	X: ND Y: ND Z:-10.1±0.21	X: ND Y: ND Z:15.71±0.1537	X: ND Y: ND Z:-3.16±0.018
260	X:10.77±0.0221 Y:7.96±0.0068 Z: ND	X: 98.91±0.1425 Y: 98.03±0.0458 Z: 96.98±0.1960	X:26.87±0.1337 Y:21.62±0.0331 Z: 2.96±0.6700	X:33.41±0.0385 Y:25.24±0.0092 Z:ND	X:ND Y: ND Z:12.32±0.172	X: ND Y: ND Z:-37.2±0.17	X: ND Y: ND Z:20.66±0.2636	X: ND Y: ND Z:-7.7±0.2772
264	X:6.62±0.0221 Y:14.87±0.0599 Z: ND	X: 101.29±0.1619 Y: 96.82±0.3005 Z: 99.18±0.6534	X:26.56±0.1717 Y:16.35±0.1632 Z: 2.54±1.7962	X:32.40±0.0173 Y:24.75±0.0194 Z:ND	X:ND Y: ND Z:31.44±0.778	X: ND Y: ND Z:-41.5±0.53	X: ND Y: ND Z:27.92±0.7095	X: ND Y: ND Z:-13.59±0.14
267	X:8.82±0.0027 Y:23.74±0.0371 Z: ND	X: 103.19±0.0372 Y: 91.84±0.4343 Z: 98.34±1.25	X:34.05±0.0098 Y:38.32±0.0746 Z: -6.50±0.7766	X:36.91±0.0081 Y:40.44±0.0539 Z:ND	X:ND Y: ND Z:22.89±0.627	X: ND Y: ND Z:-31.1±0.95	X: ND Y: ND Z:11.53±0.5567	X: ND Y: ND Z:-6.59±0.185
276	X:5.26±0.0076 Y:30.87±0.5372 Z: ND	X: 85.05±0.2649 Y: 91.13±0.9410 Z: 88.07±0.8951	X: 4.37±0.0787 Y: 0.79±1.2310 Z: -10.25±0.501	X:10.14±0.0136 Y:28.61±0.3511 Z:ND	X:ND Y: ND Z:17.66±0.292	X: ND Y: ND Z:-8.54±0.54	X: ND Y: ND Z:2.78±0.1828	X: ND Y: ND Z:-6.36±0.108
277	X:3.53±0.0025 Y:10.35±0.0045 Z: ND	X: 101.67±0.0403 Y: 101.66±0.0156 Z: 88.97±1.3851	X:32.96±0.0901 Y:18.38±0.0305 Z: -14.02±0.53	X:35.44±0.0282 Y:25.48±0.0167 Z:ND	X:ND Y: ND Z:19.18±0.495	X: ND Y: ND Z:-22.3±0.67	X: ND Y: ND Z: 4.09±0.5282	X: ND Y: ND Z:-8.69±0.16
284	X:7.08±0.0302 Y:10.31±0.0084 Z: ND	X: 96.59±0.3143 Y: 98.52±0.1048 Z: 97.7±0.5849	X:21.8±0.2322 Y:13.48±0.0723 Z: 5.60±0.5677	X:28.63±0.0219 Y:17.62±0.0073 Z:ND	X:ND Y: ND Z:16.56±0.726	X: ND Y: ND Z:-20.9±0.14	X: ND Y: ND Z: 25.08±0.41	X: ND Y: ND Z:-5.6±0.081

REFERENCES

[1] F. G. Yanowitz, *Introduction to ECG Interpretation V8.0*, Booklet IHC ECG Services, LDS Hospital & Intermountain Medical Center, pp. 1-83, July 2012.

[2] R. L. Avitia, M. A. Reyna, M. E. Bravo, and L. A. Cetto, "QRS Complex duration enhancement as ventricular late potential indicator by signal/averaged ECG using time-amplitude alignments," *Biomed Eng-Biomed Te.*, vol. 58, pp. 179-186, 2013.

[3] M. B. Conover, *Understanding Electrocardiography*, 8th ed. St Louis, MO: Mosby, 2003.

[4] R. N. Carol, "ECG Challenges: Myocardial Infarction Mimics Q Wave," *AACN Advanced Critical Care*, vol. 18, no. 4, pp. 440-444, 2007.

[5] J. M. N. Carol, "RN, ECG Challenges: Myocardial Infarction Mimics ST segments," *AACN Advanced Critical Care*, vol. 19, no. 2, pp. 245-248, 2008.

[6] A. L. Goldberger, L. A. Amaral, L. Glass, J. M. Hausdorff, P. C. Ivanov, R. G. Mark, J. E. Mietus, G. B. Moody, C. K. Peng, and H. E. Stanley, "Physiobank, Physiobank, and Physionet: Components of a new research resource for complex physiologic signals," *Circulation*, vol. 101, no. 23, 2000.

[7] J. Pan and W. J. Tompkins, "A real time QRS detection algorithm," *IEEE Trans Biomed Eng.*, vol. 32, issue 3, pp. 230-236, 1985.

- [8] D. Benitez and F. M. Tipan, "Desarrollo e Implementacion de un algoritmo para la caracterizaci3n de los limites de una forma de onda de un electrocardiograma (ECG) utilizando ondillas (wavelets)," *JIEE*, vol. 19, 2005.



**Manuel M. Casas** received the B.S degree in bioengineering and biomedical instrumentation specialization from the Autonomous University of Baja California (UABC), M3xico in 2014. His past employment includes researcher assistant at National Institute of Astrophysics, Optics, and electronics and biomedical engineer at General Hospital of Mexicali.

Mr. Martinez is currently a research-engineer partner at Mexican-Europe Institute of Sciences. His interests include development of medical instrumentation and clinical research.



**Roberto L. Avitia** received the B.S degree in biomedical electronic engineering from General Administration of Technological Institutes, Mexico in 2004, the M.S. degree in bioelectronics from the Center for Research and Advanced Studies of the National Polytechnic Institute, Mexico in 2006 and the Ph.D. degree in engineering from Autonomous University of Baja California (UABC), Mexico in 2013. His past employment includes industrial at Hirata Engineering

and hospital experience at National Institute of Cardiology.

He joined the Department of Bioengineering and Environmental Health at UABC in 2007 by applying dynamic programming and machine learning algorithms in high resolution electrocardiography (HRECG). He was creator of the bioengineering undergraduate program at UABC.

Dr. L. Avitia is currently a full professor of the bioengineering program of the UABC and member of the National System of Researchers. His research interests include not-linear modelling of HRECGs, development of medical instrumentation, and pattern recognition in biomedical images.



**Alexandra Gomez-Caraveo** is currently a last-year student for bioengineering and biomedical instrumentation specialization at Autonomous University of Baja California, M3xico. Her past employment includes researcher assistant in a Biology Laboratory of University of Guanajuato and biomedical engineering support at hospital ISSSTE CALI.

Miss Gomez-Caraveo is currently working in a research project titled "analysis of arrhythmias in standard electrocardiography". Her research

interests include biomedical instrumentation and biomedical digital signal processing.



**Marco A. Reyna** received the B.S. degree in electrical engineering from Autonomous University of Baja California (UABC)-Mexicali, Mexico, in 1990. Received the M.S. (Hon) degree in biomedical engineering from Metropolitan Autonomous University-Mexico D.F., in 1994, and the Ph.D. (Cum Laude) degree in bioengineering from the Polytechnic University of Catalunya, Barcelona, Spain, in 1998.

From 1988 to 1989, he was an electrical technician at the International Circuits enterprise in Mexicali, B.C., Mexico, where he performed the electrical test of different electronic products.

In 1989 he was hired by the UABC, in Baja California, Mexico, where he has taught undergraduate and graduate courses, managed several research projects, published scientific articles in various journals, published book chapters, and a book, all related to bioengineering and environmental health. He was the creator of the bioengineering and environmental health laboratory, creator of the bioengineering undergraduate degree program.

Dr. Reyna is currently a full researcher at UABC, the leader of the bioengineering and environmental health research group and member of the National System of Researchers.



**Jose A. C3rdenas-Haro** received his B.S. degree in electronic engineering at the Technological Institute of Los Mochis, his M.Sc. degree in computer science at the Ensenada Center for Scientific Research and Higher Education (CICESE), and his Ph.D. degree in computer science at the Arizona State University (ASU). His research interests include parallel and distributed computing, network security,

bioinformatics and applied mathematics. He is currently working as a full time professor at the Autonomous University of Baja California (UABC).